

MASTER THESIS (2017-2018)

INTERNSHIP REPORT

Effect of magnetic field in square and honeycomb lattice

Supervisor:

Prof. Guy Trambly
Javad Vahedi

Institute:

University de Cergy
Pontoise

Candidate:

Maheshwor Tiwari

June 23, 2018



Acknowledgements

It has been a privilege for me doing the internship with financial support from University de Cergy Pontoise. I would like to thank my supervisors Prof. Guy Trambly and Javad Vahedi for guiding throughout the internship period. I would like to extend special thanks to my supervisor Javad Vahedi for giving full attention to my work and guiding me through whenever it was necessary. I am very grateful for his remarkable advice, his physical insights as well as for the freedom he gave me, allowing me to learn and grow without pressure. I am particularly thankful to Prof. Andreas Honecker for providing this opportunity to be the part of research team as an intern. I am grateful for his support throughout the master program , for the suggestions and the many helpful scientific discussion and also for the moral support.

Abstract

This thesis reports on effect of magnetic field on 2D materials like square lattice and honeycomb lattice. We review some of the most relevant methods used for the implementation of effect of magnetic field on different lattices. The effect of magnetic field is well explained in terms of Peierls substitution. While some of the effects of electromagnetism are familiar even to non-physicists, and most of the surprising phenomena arising from gauge fields are only understood through quantum mechanical concepts. For example, when a free electron is immersed in a uniform magnetic field, its quantum- mechanical energy splits into equally-spaced Landau levels. Such energy quantization exist no more in any classical calculation and it provides a nice explanation of the integer quantum Hall effect. That is quantization occur at low temperature and strong magnetic field. If we consider an electron on a crystal lattice which is placed in high magnetic field, the effect on Bloch bands and Landau levels results in a beautiful fractal self-recursive energy spectrum, which is known as Hofstadter Butterfly. Moreover, this structure is generally obtained by diagonalizing the Harper equation. Basically, we work on square lattice and honeycomb lattice with nearest neighbour consideration. Then, we applied magnetic field on 2D lattice and analyze its effect. This thesis provides the basic insights to extend the research work for next nearest neighbour interaction under the effect of magnetic field.

Contents

Acknowledgements	i
Abstract	ii
1 Effect of magnetic field in a square lattice	1
1.1 Introduction	1
1.2 Hamiltonian and Peierls Phase	1
1.3 Magnetic Translation Operators	3
1.4 Supercell and Magnetic unit cell	6
1.5 Magnetic traslation operator for $\alpha = \frac{1}{q}$	8
1.6 Diagonalization of the Hamiltonian of a 2D Square Lattice in a Magnetic Field . .	11
1.7 Particle hole symmetry	13
1.8 Hofstadter Butterfly in square lattice	14
2 Honeycomb lattice	17
2.1 Honeycomb lattice without magnetic field	17
2.2 Honeycomb lattice in a magnetic field	21
2.3 Hofstadter butterfly in a Honeycomb Lattice	23
2.4 Hofstadter butterfly in a tunable optical lattice	24
3 Berry Curvature, Berry Phase,Chern Number	27
3.1 Introduction	27
3.2 Chern Number and Hall conductance	28
3.3 The Diophantine equation	28
4 Future Work	32
Summary	34

List of Figures

1.1	Schematic diagram of square lattice in which hopping parameter t is determined by Peierls phase.	2
1.2	Magnetic unit cells of a square lattice. Schematic drawing of a square lattice with lattice constant a . The area of the magnetic unit cell (green shaded area) depends on the magnetic flux. There are three different possibilities to choose its shape: a) rectangular and oriented along y axis, b) symmetric c) rectangular and oriented along x axis	8
1.3	Energy band diagram of the square lattice without magnetic field.	10
1.4	Contour plot of energy band in case of square lattice	11
1.5	Hofstadter butterfly calculated for the Square lattice for $q=251$	14
1.6	Single particle energy spectrum of the Hofstadter model in the unit of t as a function of k_x and k_y in the magnetic Brillouin zone for $\Phi = 1/2, 1/3$ and $1/3$ respectively. For respective values of Φ the spectrum splits into 2, 3, and 4 subbands respectively.	15
2.1	Honeycomb lattice with primitive vectors	17
2.2	Energy-band diagram of honeycomb lattice.	20
2.3	Contour plot of energy band for Honeycomb lattice	20
2.4	Magnetic unit cell in Honeycomb lattice	21
2.5	Hofstadter butterfly calculated for the Honeycomb lattice for $q=251$	24
2.6	Tunable optical lattice	25
2.7	Hofstadter Butterfly in a Tunable lattice.	25
3.1	Chern number representation in square Hofstadter butterfly at different values of Φ . The x -axis represents magnetic flux and y -axis represents Energy.	31
3.2	Chern Number representation in honeycomb Hofstadter butterfly at different values of Φ . The y -axis represents magnetic flux and x -axis represents Energy.	31
4.1	The colored butterfly, [29], shows energy gaps colored according to the quantized values of the Hall conductance. Warm colors indicate positive chern numbers, and cool colors negative. The x -axis represents magnetic flux and y -axis represents Energy.	32
4.2	The colored butterfly, [30], shows energy gaps colored according to the quantized values of the Hall conductance. Warm colors indicate positive Chern numbers, and cool colors negative. The x -axis represents magnetic flux and y -axis represents Energy.	33

Chapter 1

Effect of magnetic field in a square lattice

1.1 Introduction

In the presence of periodic potential, electrons experience a quantized energy spectrum where the discrete energy bands are called Bloch Bands. On applying the magnetic field, one observes degeneracy in the energy levels. We present a details of the problem of a 2-D lattice in the presence of uniform magnetic field using Peierls phase. By such consideration we learn about magnetic translation operators, the Hofstadter problem, particle hole symmetry with some brief discussion about chern number.

1.2 Hamiltonian and Peierls Phase

We take spinless electrons and want to analyze simplest nontrivial, tight binding Hamiltonian. For a single electron in 2D lattice potential the Hamiltonian contains only kinetic term and can be written as;

$$H_0 = -t \sum_{m,n} (\hat{a}_{m+1,n}^\dagger \hat{a}_{m,n} + \hat{a}_{m,n+1}^\dagger \hat{a}_{m,n} + h.c) \quad (1.1)$$

where, t is hopping parameter which determines an electron to hop from one atom to other, $\hat{a}_{m,n}^\dagger, \hat{a}_{m,n}$ are creation and annihilation operators on site (m, n) respectively. m is site index along x axis and n is site index along y axis.

The model is based on the tight-binding approximation (TBA) where the electrons are assumed to occupy the standard orbitals of the atoms and overlap between atomic wave functions on neighbouring sites is small [1]. In other words, TBA defines a system having a discrete lattice and electron can only stay on lattice site.



In the presence of magnetic field $\mathbf{B} = \nabla \times \mathbf{A}$, \mathbf{A} is vector potential, equation 1.1 can be modified according to Peierls substitution [1].

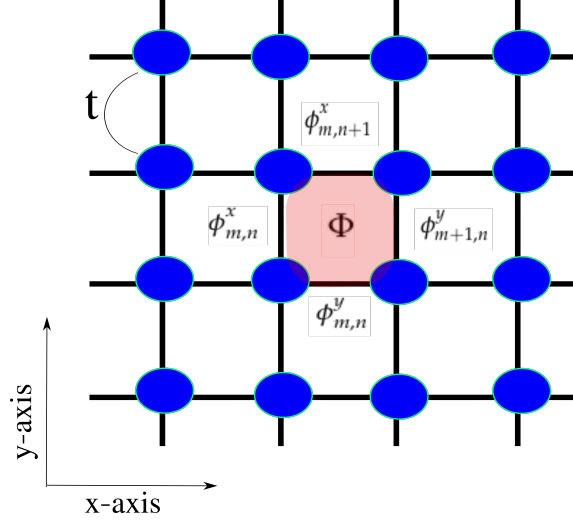


Figure 1.1: Schematic digram of square lattice in which hopping parameter t is determined by Peierls phase.

Then, hopping parameter is accompanied by Peierls phase

$$\phi_{m,n}^i = \frac{-eA_{m,n}^i}{\hbar} \quad (1.2)$$

where $i = \{x, y\}$, e is the electronic charge and \hbar is Planck's constant.

Now, in the presence of magnetic field, the Hamiltonian acquire the phase which can be written as;

$$\hat{H} = -t \sum_{m,n} (e^{i\phi_{m,n}^x} \hat{a}_{m+1,n}^\dagger \hat{a}_{m,n} + e^{i\phi_{m,n}^y} \hat{a}_{m,n+1}^\dagger \hat{a}_{m,n} + h.c) \quad (1.3)$$

Invoking Aharonov-Bohm effect which is a quantum mechanical phenomenon in which an electrically charged particle affects electromagnetic potential, despite being confine to a region in which both magnetic and electric field are zero [3]. Since the Hamiltonian contains only nearest neighbour terms, then using Aharonov-Bohm effect the phase factors can be choosen as the integral of the external vector potential over the bond linking the nearest neighbours. So, Aharonov-Bohm phase Φ_{AB} is,

$$\Phi_{AB} = -\frac{e}{\hbar} \oint_c \vec{A} \cdot d\vec{r} = -\frac{e}{\hbar} 2\pi \oint_c \vec{A} \cdot d\vec{r} = -2\pi \frac{h}{e} \Phi = -2\pi \frac{\Phi}{\Phi_0} \quad (1.4)$$



where Φ is the magnetic flux through the area enclosed by the contour C and Φ_0 is the magnetic quantum flux.

Now, magnetic flux per unit cell can be defined as,

$$\alpha = \frac{1}{2\pi}\Phi = \frac{1}{2\pi}(\phi_{m,n}^x + \phi_{m+1,n}^y - \phi_{m,n+1}^x - \phi_{m,n}^y) \quad (1.5)$$

In general, Φ will be denoted as flux per unit cell.

1.3 Magnetic Translation Operators

In the absence of magnetic field, lattice translation operator can be defined as,

$$\begin{aligned} \hat{T}_x^0 &= \sum_{m,n} \hat{a}_{m+1,n}^\dagger \hat{a}_{m,n} \\ \hat{T}_y^0 &= \sum_{m,n} \hat{a}_{m,n+1}^\dagger \hat{a}_{m,n} \end{aligned} \quad (1.6)$$

These lattice translation operators commute with the Hamiltonian $[\hat{T}_{x,y}^0, \hat{H}_0] = 0$ and also commute with each other $[\hat{T}_x^0, \hat{T}_y^0] = 0$. In the absence of magnetic field, these operators translate by one lattice unit vector and Hamiltonian is invariant under the translation. However, in the presence of magnetic field, there exist a vector potential $A_{m,n}$ which is not translational invariant because its presence perturbs the periodicity of the lattice. Consequently, the Hamiltonian is not invariant under lattice translation. In the presence of magnetic field, Hamiltonian need to be modified as equation 1.3. So, we need another sets of translation operator defined as,

$$\begin{aligned} \hat{T}_x &= \sum_{m,n} \hat{a}_{m+1,n}^\dagger \hat{a}_{m,n} e^{i\phi_{m,n}^x} \\ \hat{T}_y &= \sum_{m,n} \hat{a}_{m,n+1}^\dagger \hat{a}_{m,n} e^{i\phi_{m,n}^y} \end{aligned} \quad (1.7)$$

Let's check the symmetries of the Hamiltonian. We clearly see that translation operators do not commute. For example, when we act on a single-particle state at site (m, n) $|\psi_{m,n}\rangle$

$$\begin{aligned} \hat{T}_x \hat{T}_y \psi_{m,n} &= \hat{T}_x e^{i\phi_{m,n}^y} \psi_{m,n+1} = e^{i\phi_{m,n+1}^x + i\phi_{m,n}^y} \psi_{m+1,n+1} \\ \hat{T}_y \hat{T}_x \psi_{m,n} &= \hat{T}_y e^{i\phi_{m,n}^x} \psi_{m+1,n} = e^{i\phi_{m+1,n}^y + i\phi_{m,n}^x} \psi_{m+1,n+1} \\ \hat{T}_y \hat{T}_x \psi_{m,n} &= e^{i2\pi\phi_{m,n}} \hat{T}_x \hat{T}_y \psi_{m,n} \end{aligned} \quad (1.8)$$

So, in an external, constant magnetic field, we see that the Hamiltonian is not translationally in-



variant because the two translation operators do not commute with each other $[\hat{T}_x, \hat{T}_y] \neq 0$ (hence do not commute with the Hamiltonian $[\hat{T}_{x,y}, \hat{H}] \neq 0$). Although the homogeneous magnetic field is invariant, but we can not be sure vector potential will be invariant because of broken periodicity due to presence of magnetic field. A gauge transformation is required to make the Hamiltonian translationally invariant, but we cannot maintain the translational symmetry of the original lattice [2].

We are more interested in the translational invariance again. We want the periodicity back through some new sorts of translational operators. Through these operators we find new symmetries of the lattice Hamiltonian in the presence of flux in such a way to recover translational invariance. These new set of operators are called Magnetic Translation operators (MTOs) and given as,

$$\begin{aligned}\hat{T}_x^M &= \sum_{m,n} \hat{a}_{m+1,n}^\dagger \hat{a}_{m,n} e^{i\theta_{m,n}^x} \\ \hat{T}_y^M &= \sum_{m,n} \hat{a}_{m,n+1}^\dagger \hat{a}_{m,n} e^{i\theta_{m,n}^y}\end{aligned}\tag{1.9}$$

These operators have to be one body operators because we are solving a one-body Hamiltonian. Also, their phase have to be different from the original ones, because previously translation operators do not commute. These MTOs acquired the phase $\theta_{m,n}^i$. The choice of phase $\theta_{m,n}^i$ is tricky and need to be chosen in such a way that MTOs commute with the Hamiltonian defined in equation 1.3, i.e. $[\hat{T}_i^M, \hat{H}] = 0$.

So, we require $[\hat{T}_x^M, \hat{H}] = 0$ and $[\hat{T}_y^M, \hat{H}] = 0$ where $\hat{H} = \hat{T}_x + \hat{T}_y + h.c.$

such that, $[\hat{T}_x^M, \hat{T}_x + \hat{T}_x + h.c.] = 0$

That means, each relation, $[\hat{T}_x^M, \hat{T}_x]$, $[\hat{T}_x^M, \hat{T}_y]$, $[\hat{T}_y^M, \hat{T}_x]$, $[\hat{T}_y^M, \hat{T}_y]$ has to be zero.

$$\begin{aligned}[\hat{T}_x^M, \hat{T}_x] &= \sum_{m,n} [e^{i(\theta_{m+1,n}^x + \phi_{m,n}^x)} - e^{i(\phi_{m+1,n}^x + \theta_{m,n}^x)}] \psi_{m+2,n} \\ &= \sum_{m,n} e^{i(\theta_{m+1,n}^x + \phi_{m,n}^x)} [1 - e^{i(\phi_{m+1,n}^x - \phi_{m,n}^x - \theta_{m+1,n}^x + \theta_{m,n}^x)}] \psi_{m+2,n} \\ &= \sum_{m,n} e^{i(\theta_{m+1,n}^x + \phi_{m,n}^x)} [1 - e^{i(\Delta_x \phi_{m,n}^x - \Delta_x \theta_{m,n}^x)}] \psi_{m+2,n}\end{aligned}\tag{1.10}$$

We introduce lattice derivatives

$$\begin{aligned}\Delta_x \theta_{m,n}^x &= \theta_{m+1,n}^x - \theta_{m,n}^x \\ \Delta_x \phi_{m,n}^x &= \phi_{m,n+1}^x - \phi_{m,n}^x\end{aligned}\tag{1.11}$$



For $[\hat{T}_x^M, \hat{T}_x] = 0$, following relation need to be satisfied.

$$\Delta_x \phi_{m,n}^x = \Delta_x \theta_{m,n}^x \quad (1.12)$$

Similarly, for $[\hat{T}_x^M, \hat{T}_y]$ to be equal to zero, following relation need to be satisfied as we discussed above,

$$\Delta_y \theta_{m,n}^x = \Delta_x \phi_{m,n}^y \Delta_x \phi_{m,n}^y = \Delta_y \phi_{m,n}^x + \phi_{m,n} \quad (1.13)$$

Also, for $[\hat{T}_y^M, \hat{T}_x] = 0$ we obtain

$$\Delta_y \phi_{m,n}^x = \Delta_x \theta_{m,n}^y \Delta_x \theta_{m,n}^y = \Delta_x \phi_{m,n}^y - \phi_{m,n} \quad (1.14)$$

And, for $[\hat{T}_y^M, \hat{T}_y] = 0$ we have

$$\Delta_y \theta_{m,n}^y = \Delta_y \phi_{m,n}^y \quad (1.15)$$

For equations 1.13 and 1.14 equation 1.5 has been used.

Equations 1.12, 1.13, 1.14 and 1.15 can be solved to obtain new phase according as,

$$\begin{aligned} \theta_{m,n}^x &= \phi_{m,n}^x + \Phi_{m,n} \quad n \\ \theta_{m,n}^y &= \phi_{m,n}^y - \Phi_{m,n} \quad m \end{aligned} \quad (1.16)$$

Hence, we have now found operators that commute with H but do not commute between themselves: i.e. $[\hat{T}_x^M, \hat{T}_y^M] \neq 0$ when we act on a single-particle state at site (m, n) $|\psi_{m,n}\rangle$

$$\begin{aligned} \hat{T}_x^M \hat{T}_y^M \psi_{m,n} &= e^{i(\theta_{m,n+1}^x + \theta_{m,n}^y)} \psi_{m+1,n+1} \\ \hat{T}_y^M \hat{T}_x^M \psi_{m,n} &= e^{i(\theta_{m,n}^x + \theta_{m+1,n}^y)} \psi_{m+1,n+1} \end{aligned} \quad (1.17)$$

If we consider homogeneous magnetic field with $\Phi_{m,n} \equiv \Phi = 2\pi\alpha$ per unit cell. Then, we can obtain the combined relation for equations 1.17 as,

$$e^{-i\Phi} \hat{T}_x^M \hat{T}_y^M = \hat{T}_y^M \hat{T}_x^M \quad (1.18)$$

From this relation we can see that MTOs will commute with each other if Φ is integer multiple of 2π . This equation also illustrate that MTO acts on a single particle state $\psi_{m,n}$ around the border of one lattice unit cell.



1.4 Supercell and Magnetic unit cell

From equation 1.18, if the values of $\Phi = \nu \times 2\pi, \nu \in Z$, is different from integer multiple of 2π , then, we can construct magnetic translation operators for a super cell of dimension $k \times l$ in which lattice is pierced by magnetic flux which is equal to an integer multiple of 2π . So, consequently we can construct MTO that acts on border of super cell.

Recalling equations 1.9 ,

$$\begin{aligned}\hat{T}_x^M &= \sum_{m,n} \hat{a}_{m+1,n}^\dagger \hat{a}_{m,n} e^{i\theta_{m,n}^x} \\ \hat{T}_y^M &= \sum_{m,n} \hat{a}_{m,n+1}^\dagger \hat{a}_{m,n} e^{i\theta_{m,n}^y}\end{aligned}$$

Now for a super cell,

$$\begin{aligned}(\hat{T}_x^M)^k (\hat{T}_y^M)^l &= (\hat{T}_x^M)^k (\hat{a}_{m,n+1}^\dagger \hat{a}_{m,n} e^{i\theta_{m,n}^y})^l \psi_{m,n} \\ &= (\hat{T}_x^M)^K \exp\left(i \sum_{\nu=0}^{l-1} \theta_{m,n+\nu}\right) \psi_{m,n+l} \\ &= (\hat{a}_{m+1,n} \hat{a}_{m,n} e^{i\theta_{m,n}^x})^k \exp\left(i \sum_{\nu=0}^{l-1} \theta_{m,n+\nu}\right) \psi_{m,n+l} \\ &= \exp\left(i \sum_{\mu=0}^{k-1} \theta_{m+\mu,n+l} + i \sum_{\nu=0}^{l-1} \theta_{m,n+\nu}\right) \psi_{m+k,n+l}\end{aligned}$$

Similarly,

$$\begin{aligned}(\hat{T}_y^M)^l (\hat{T}_x^M)^k &= (\hat{T}_y^M)^l \exp\left(i \sum_{\mu=0}^{k-1} \theta_{m+\mu,n}^x\right) \psi_{m+k,n} \\ &= \exp\left(i \sum_{\nu=0}^{l-1} \theta_{m+k,n+\nu} + i \sum_{\mu=0}^{k-1} \theta_{m+\mu,n}\right) \psi_{m+k,n+l}\end{aligned}$$

Remarks: From the above equations, total phase acquired by single particle state $\psi_{m,n}$ along the border of super cell which is translated with MTOs is sum of corresponding phase term $\theta_{m,n}^i$ along the border of super cell. Now, for a given super cell, equation 1.18 can be written as,

$$e^{-ikl\Phi} (\hat{T}_x^M)^k (\hat{T}_y^M)^l = (\hat{T}_y^M)^l (\hat{T}_x^M)^k \quad (1.19)$$



Commutator vanishes if $\Phi = \nu \times 2\pi, \nu \in Z$. For $\nu = \frac{p}{q}$, rational value such that, $\Phi = 2\pi \frac{p}{q}$. It vanishes for $kl\Phi = 2\pi \frac{p}{q} kl$ i.e. for $kl = q$

For $kl = q$ we get smallest possible super cell in which $[(\hat{T}_x^M)^k (\hat{T}_y^M)^l] = 0$. Such type of super cell is called Magnetic unit cell.

Remarks: Area of magnetic unit cell = $q \times$ area of normal lattice cell containing q sites .

Let us define new set of operators for super cell as,

$$(\hat{T}_x^M)^k = \hat{M}_x^k (\hat{T}_y^M)^l = \hat{M}_y^l \quad (1.20)$$

The new operators in equation 1.20 along with the Hamiltonian defined by equation 1.3 form a complete set of commuting operators such tha one can find simultaneous eigenstates $\psi_{m,n}$ by formulating a generalized Bloch theorem based on magnetic translation symmetries [1]. Invoking Bloch theorem for new set of operators,

$$\begin{aligned} \hat{M}_x^k \psi_{m,n} &= e^{ik_x ka} \psi_{m,n} \\ \hat{M}_y^l \psi_{m,n} &= e^{ik_y la} \psi_{m,n} \end{aligned} \quad (1.21)$$

Also, we have the relation [1]

$$\begin{aligned} \hat{M}_x^k \psi_{m,n} &= e^{i\mu_{m,n}^x} \psi_{m+k,n} \\ \hat{M}_y^l \psi_{m,n} &= e^{i\mu_{m,n}^y} \psi_{m,n+l} \end{aligned} \quad (1.22)$$

where $kl = q$, a is lattice constant,

$\vec{k} = (k_x, k_y)$ defined in FBZ $-\frac{\pi}{ka} \leq k_x < \frac{\pi}{ka}$ and $-\frac{\pi}{la} \leq k_y < \frac{\pi}{la}$

$$\begin{aligned} \mu_{m,n}^x &= \sum_{\mu=0}^{k-1} \theta_{m+\mu,n}^x \\ \mu_{m,n}^y &= \sum_{\nu=0}^{l-1} \theta_{m,n+\nu}^y \end{aligned}$$

Remarks: The area of magnetic unit cell is fixed by the strength of the magnetic flux $\alpha = \frac{p}{q}$. The dimension of magnetic unit cell, however, are not [1].



1.5 Magnetic translation operator for $\alpha = \frac{1}{q}$

Earlier we discussed that Magnetic translation operator do not commute with each other. However, they commute with the Hamiltonian define in equation 1.3. In general, we can find a combination of the translation operators that does commute with each other. For that to happen, it depends upon the gauge that we use in particular. i.e. $\phi_{m,n} = (-2\pi\alpha n, 0)$ where α is uniform magnetic flux per unit cell [1]. So, recalling equation 1.18

$$e^{-i\Phi} \hat{T}_x^M \hat{T}_y^M = \hat{T}_y^M \hat{T}_x^M$$

Here we are considering the special case for magnetic translation operator for $\alpha = \frac{1}{q}$. This choice suggests that the magnetic unit cell consists of q lattice unit cells such that area of magnetic unit cell is q times the area of lattice unit cell. For a given value of magnetic flux, there are different possibilities to choose its dimensions [1].

Let us consider a special case where $\alpha = \frac{1}{4}$. In this case the area of magnetic unit cell is $4a^2$, where a is lattice constant. So, we have three possibilities of choosing dimension of magnetic unit cell which are illustrated in figure 1.2

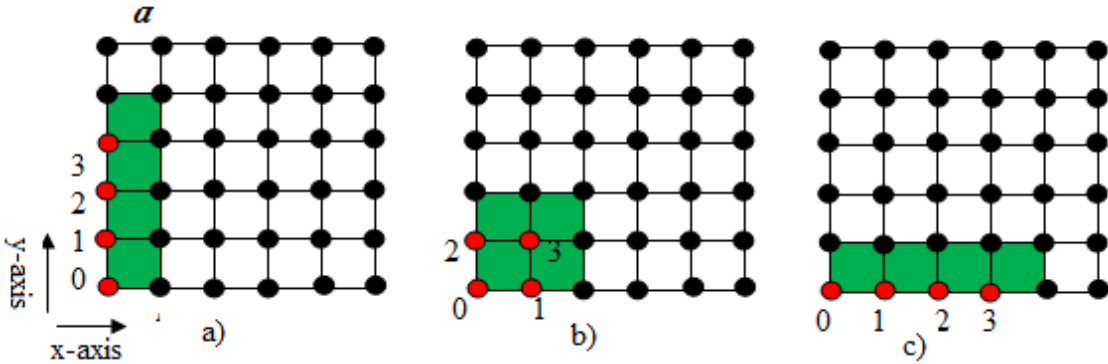


Figure 1.2: Magnetic unit cells of a square lattice. Schematic drawing of a square lattice with lattice constant a . The area of the magnetic unit cell (green shaded area) depends on the magnetic flux. There are three different possibilities to choose its shape: a) rectangular and oriented along y axis, b) symmetric c) rectangular and oriented along x axis

For further calculations, we will take the first case where we are dealing with a magnetic unit cell oriented along y direction. With this it can be inferred that Magnetic translation operator along x corresponds to translation by one lattice constant and along y corresponds to translation by q lattice constants.

Now, for this particular case, the translation operator for magnetic unit cell can be written as,



$$\begin{aligned}
 \hat{M}_x^1 &= \sum_{m,n} \hat{a}_{m+1,n}^\dagger \hat{a}_{m,n} \\
 \hat{M}_y^q &= \sum_{m,n} \hat{a}_{m,n+q}^\dagger \hat{a}_{m,n} e^{-2i\pi\alpha ml} \\
 &= \sum_{m,n} \hat{a}_{m,n+4}^\dagger \hat{a}_{m,n}
 \end{aligned} \tag{1.23}$$

Where we use $k l = 1a \times 4a$, $\alpha = \frac{1}{q}$

Invoking Bloch Theorem,

$$\hat{M}_x^1 \psi_{m,n} = e^{ik_x a} \psi_{m,n}$$

where,

$$\hat{M}_x^1 \psi_{m,n} = \hat{T}_x^M \psi_{m,n} = \hat{a}_{m+1,n}^\dagger \hat{a}_{m,n} \psi_{m,n} = \psi_{m+1,n} \tag{1.24}$$

So, we have,

$$\hat{M}_x^1 \psi_{m,n} = e^{ik_x a} \psi_{m,n} = \psi_{m+1,n} \tag{1.25}$$

Also,

$$\hat{M}_y^q \psi_{m,n} = e^{4ik_x a} \psi_{m,n}$$

where,

$$\hat{M}_y^q \psi_{m,n} = (\hat{T}_y^M)^l \psi_{m,n} = \psi_{m,n+q}$$

$$\hat{M}_y^q \psi_{m,n} = e^{4ik_x a} \psi_{m,n} = \psi_{m,n+q} \tag{1.26}$$

1.5.1 Energy dispersion in the absence of magnetic field

When there is no magnetic field applied in the system, we obtain energy dispersion relation. In this case, Harper-Hofstadter Hamiltonian defined in equation 1.3 becomes,

$$\hat{H} = -t \sum_{m,n} (\hat{a}_{m+1,n}^\dagger \hat{a}_{m,n} + \hat{a}_{m,n+1}^\dagger \hat{a}_{m,n} + h.c) \tag{1.27}$$



Making use of Fourier transform,

$$\begin{aligned}\hat{a}_{m,n} &= \frac{1}{\sqrt{N}} \sum_k e^{ik_x m + ik_y n} \hat{a}_{k_x k_y} \\ \hat{a}_{m,n}^\dagger &= \frac{1}{\sqrt{N}} \sum_k e^{-ik_x m - ik_y n} \hat{a}_{k_x k_y}^\dagger\end{aligned}\quad (1.28)$$

So,

$$\begin{aligned}H &= -t(e^{-ik_x a} + e^{-ik_y a} + e^{ik_x a} + e^{ik_y a}) \hat{a}_{k_x k_y}^\dagger \hat{a}_{k_x k_y} \\ H &= -t(2\cos k_x a + 2\cos k_y a) \hat{a}_{k_x k_y}^\dagger \hat{a}_{k_x k_y}\end{aligned}\quad (1.29)$$

Energy dispersion relation for non-magnetic field,

$$E(k) = -2\cos k_x a - 2\cos k_y a \quad (1.30)$$

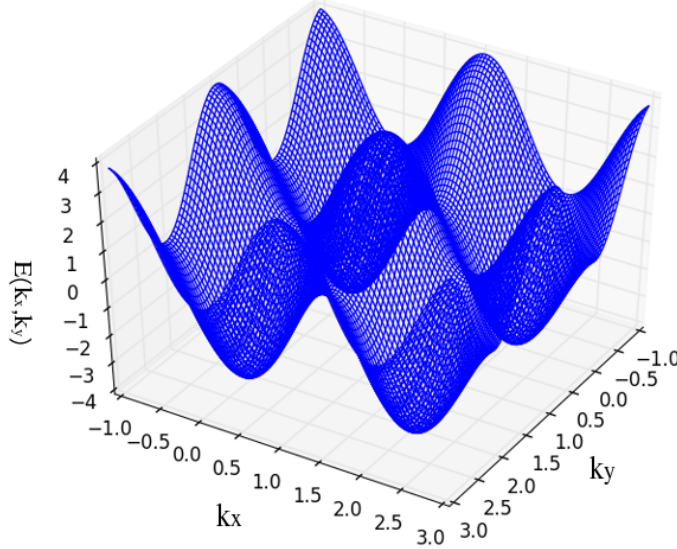


Figure 1.3: Energy band diagram of the square lattice without magnetic field.

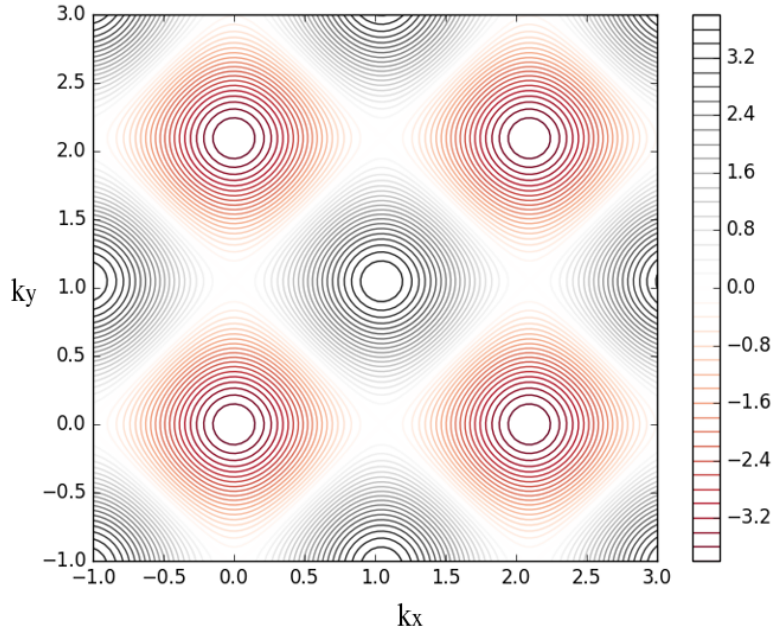


Figure 1.4: Contour plot of energy band in case of square lattice

1.6 Diagonalization of the Hamiltonian of a 2D Square Lattice in a Magnetic Field

The theoretical description of a lattice Hamiltonian with flux depends on the choice of the gauge since the explicit form of the MTOs depends on the particular form of the vector potential. [4], [5], [6]. The vector potential is written in the Landau gauge $\phi_{m,n} = (-\Phi n, 0)$. This corresponds to a uniform magnetic field with flux $\Phi = 2\pi\alpha$ per unit cell. The hamiltonian defined in this gauge is called Harper-Hofstadter Hamiltonian [4] and given as,

$$\hat{H} = -t \sum_{m,n} (e^{-i\Phi n} \hat{a}_{m+1,n}^\dagger \hat{a}_{m,n} + \hat{a}_{m,n+1}^\dagger \hat{a}_{m,n} + h.c) \quad (1.31)$$

In this gauge only tunneling along x -direction is complex while tunneling along the y -direction is real. The single particle energy spectrum obtained from this Hamiltonian provides a fractal self-similar structure as a function of the flux, known as Hofstadter's butterfly [4].

In order to solve the Schrodinger wave equation, we consider the following ansatz [1],

$$\Psi_{m,n} = e^{ik_x m a} e^{ik_y n a} \psi_n \quad (1.32)$$

where (k_x, k_y) defined in FBZ $-\frac{\pi}{a} \leq k_x < \frac{\pi}{a}$ and $-\frac{\pi}{qa} \leq k_y < \frac{\pi}{qa}$

Now solving Schrodinger wave equation,



$$E\Psi_{m,n} = H\Psi_{m,n}$$

Inserting equation 1.31 in above, we get,

$$E\Psi_{m,n} = -t \sum_{m,n} (e^{-i\Phi n} \hat{a}_{m+1,n}^\dagger \hat{a}_{m,n} + \hat{a}_{m,n+1}^\dagger \hat{a}_{m,n} + h.c) \Psi_{m,n}$$

Here we use,

$$e^{-i\Phi n} \hat{a}_{m+1,n}^\dagger \hat{a}_{m,n} \Psi_{m,n} = e^{-i\Phi n} \Psi_{m+1,n}$$

$$\hat{a}_{m,n+1}^\dagger \hat{a}_{m,n} \Psi_{m,n} = \Psi_{m,n+1}$$

$$e^{i\Phi n} \hat{a}_{m+1,n} \hat{a}_{m,n}^\dagger \Psi_{m,n} = e^{i\Phi n} \Psi_{m-1,n}$$

$$\hat{a}_{m,n+1} \hat{a}_{m,n}^\dagger \Psi_{m,n} = \Psi_{m,n-1}$$

Then we obtain following relation,

$$E\Psi_{m,n} = -t \sum_{m,n} (e^{-i\Phi n} \Psi_{m+1,n} + e^{i\Phi n} \Psi_{m-1,n} + \Psi_{m,n+1} \Psi_{m,n-1}) \quad (1.33)$$

Making use of ansatz from equation 1.32 we obtain the following relation,

$$E\psi_n = -t [(e^{i(k_x a - \Phi n)} + e^{-i(k_x a - \Phi n)}) \psi_n + e^{ik_y a} \psi_{n+1} + e^{ik_y a} \psi_{n-1}]$$

$$E\psi_n = -t [(2\cos(k_x a - \Phi n) \psi_n + e^{ik_y a} \psi_{n+1} + e^{ik_y a} \psi_{n-1})] \quad (1.34)$$

Then problem reduces to q -dimensional eigen value equation,

$$E(k) \begin{bmatrix} \psi_0 \\ \psi_1 \\ \vdots \\ \psi_{q-1} \end{bmatrix} = H(k) \begin{bmatrix} \psi_0 \\ \psi_1 \\ \vdots \\ \psi_{q-1} \end{bmatrix} \quad (1.35)$$

Consequently $q \times q$ matrix is defined as,

$$H(k) = -t \begin{bmatrix} h_0 & e^{ik_y a} & 0 & \dots & e^{-ik_y a} \\ e^{-ik_y a} & h_1 & e^{ik_y a} & \dots & 0 \\ 0 & e^{-ik_y a} & h_2 & \dots & 0 \\ \vdots & \vdots & \vdots & \ddots & \vdots \\ e^{ik_y a} & 0 & 0 & \dots & h_{q-1} \end{bmatrix} \quad (1.36)$$

with $h_q = -2t\cos(k_x a - \Phi q)$



1.7 Particle hole symmetry

Let us consider a transformation

$$\Psi_{m,n} \rightarrow \tilde{\Psi}_{m,n} (-1)^{m+n} \Psi_{m,n} \quad (1.37)$$

The new wave function satisfies the Harper equation,

$$-E\tilde{\Psi}_{m,n} = -t(e^{-i\phi n}\tilde{\Psi}_{m+1,n} + e^{i\phi n}\tilde{\Psi}_{m-1,n} + \tilde{\Psi}_{m,n+1} + \tilde{\Psi}_{m,n-1}) \quad (1.38)$$

This means if there exist a state $\Psi_{m,n}$ with energy E , then there also exists a state $\tilde{\Psi}_{m,n}$ with energy $-E$. This illustrates particle hole symmetry present in the system [1].

The new wave function can be written as,

$$\tilde{\Psi}_{m,n} = e^{ik_x m a} e^{ik_y n a} \tilde{\Psi}_n \quad (1.39)$$

where, $\tilde{\Psi}_{n+q} = \tilde{\Psi}_n$

Then, eigen value equation for new periodic wave function $\tilde{\Psi}_n$

$$-E\tilde{\Psi}_{m,n} = -t[2\cos(k_x a + \pi - \phi n)\tilde{\Psi}_n + e^{i(k_y a + \pi)}\tilde{\Psi}_{n+1} + e^{-i(k_y a + \pi)}\tilde{\Psi}_{n-1}] \quad (1.40)$$

While doing the calculation we make sure that, for the transformation from $\Psi_{m,n}$ to $\tilde{\Psi}_{m,n}$, wave vector differ by π i.e.

$$k_x a \rightarrow k_x a + \pi$$

$$k_y a \rightarrow k_y a + \pi$$

Conclusions:

1. There is shift in momentum space, on transformation of wave function $\Psi_{m,n}$ with positive energy band $E(k)$ to the wave function $\tilde{\Psi}_{m,n}$ with negative energy band $-E(k)$ such that,

$$(k_x, k_y) = (k_x + \frac{\pi}{a}, k_y + \frac{\pi}{a})$$

2. Eigen state associated with band $E(k)$ related with eigenstate associated with band $-E(k)$ by the relation,

$$\Psi_n(k_x, k_y) = \tilde{\Psi}_n(k_x + \frac{\pi}{a}, k_y + \frac{\pi}{a})$$

3. Dispersion relation of a band μ around mean energy $\bar{E}_\mu > 0$ is related to dispersion relation of a band $\tilde{\mu}$ around the mean energy $\bar{E}_{\tilde{\mu}} < 0$ as, $E_\mu(k_x, k_y) = -E_{\tilde{\mu}}(k_x + \frac{\pi}{a}, k_y + \frac{\pi}{a})$



1.8 Hofstadter Butterfly in square lattice

P.G. Harper wrote a paper [6] in 1955 in which he developed the effect of lattice potential and an external magnetic field on two dimensional square lattice. He led the foundation of Harper equation. He didn't succeed in finding the solution of his equation for different values of magnetic field. In 1976, D. Hofstadter published a paper [4] in which he found the solution of Harper equation.

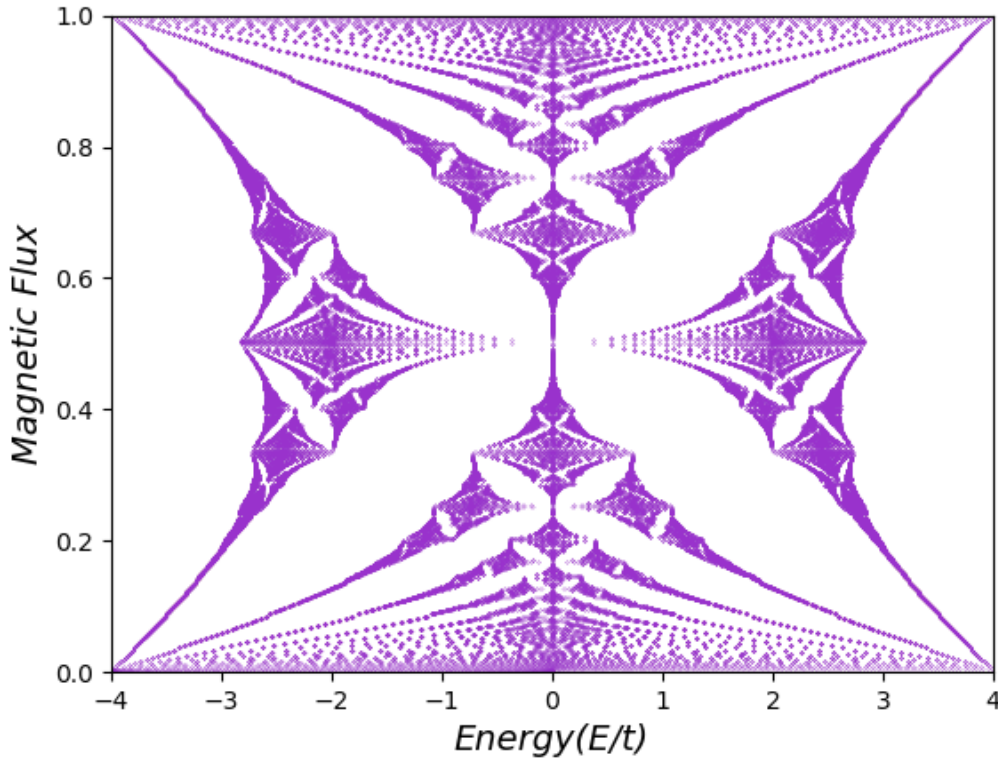
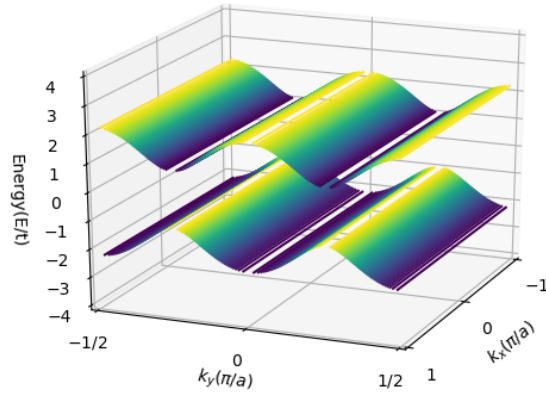
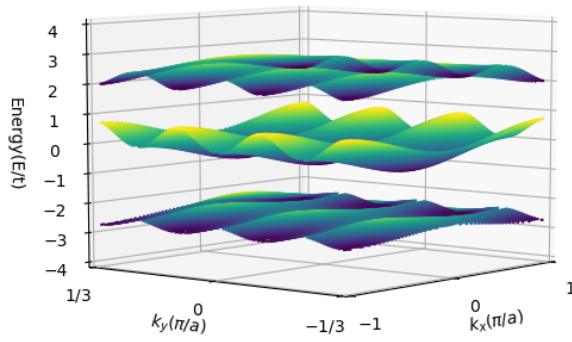


Figure 1.5: Hofstadter butterfly calculated for the Square lattice for $q=251$

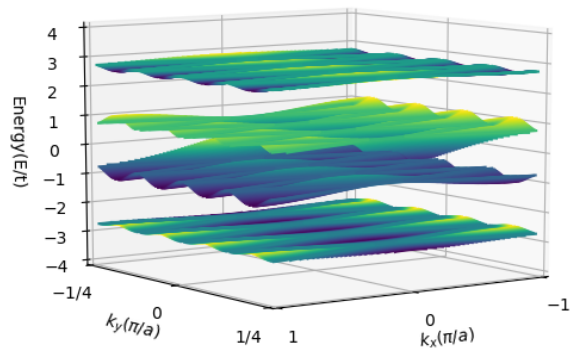
When single particle energy spectrum is plotted against the magnetic field $\Phi = \frac{p}{q}$, where p and q are mutually prime numbers, then it results self repeated, fractal structures. If suppose $\Phi = 1/3$ where $q = 3$ then, it is divided into 3 sub-bands and we will have $q-1=2$ band gap in the energy spectrum. The energy spectrum and topological properties of the system are determined by magnetic field and lattice symmetry which in turn determined by structure of unit cell [7].



[For $\Phi=1/2$]



[For $\Phi=1/3$]



[For $\Phi=1/4$]

Figure 1.6: Single particle energy spectrum of the Hofstadter model in the unit of t as a function of k_x and k_y in the magnetic Brillouin zone for $\Phi = 1/2, 1/3$ and $1/3$ respectively. For respective values of Φ the spectrum splits into 2, 3, and 4 subbands respectively.



When magnetic field is of the rational value, then, in this special case the energy spectrum divides into q bands because Harper equation is periodic with period q [8]. The energy spectrum predicted by equation 1.17 as a function of the magnetic flux Φ has a recursive and self-similar structure, which is shown in figure 1.5. The magnetic flux is plotted vertically from 0 to 1, while energy is plotted horizontally from $-4t$ to $4t$.

As we can see from the figure 1.5, for rational values of the flux $\Phi = p/q$, there must be q horizontal line segments, that represent the bands of allowed energies.

The allowed energy states of electrons confined to a 2D lattice with a perpendicular magnetic field applied. If the field is strong enough, the electrons will move in closed loops, and as they move around the loops they pick up a phase proportional to $\int_c \vec{A} \cdot d\vec{r} = \Phi$, the flux enclosed. Moreover, this structure can be used to describe the Hall conductance [9].

Chapter 2

Honeycomb lattice

2.1 Honeycomb lattice without magnetic field

The honeycomb lattice is a triangle lattice with two sites (A, B) in each unit cell. It is a bipartite lattice, which consists of two sublattices and only the inter-band hopping, ($A - B$), ($B - A$), are possible. The nn tight binding approximation does exclude ($A - A$) and ($B - B$) hopping. The electronic properties of graphene can be described using a simple TB mode. The tight binding method suggested by Bloch in 1928 consists of expanding the states of the crystal in linear combinations of atomic orbitals of the component atoms [10]. The wave function of an electron in the system can be written as a Linear Combination of Atomic Orbitals (LCAO) [11]. The Hamiltonian of such system is given by,

$$H = -t \sum_{\langle m,n \rangle} (a_m^\dagger b_n + h.c) \quad (2.1)$$

where, $\langle m, n \rangle$ denotes nearest neighbors and t is the hopping parameter between them that represents the overlap between orbitals. This Hamiltonian just describes the hopping of electrons from sublattice A to B controlled by the parameter t [13].

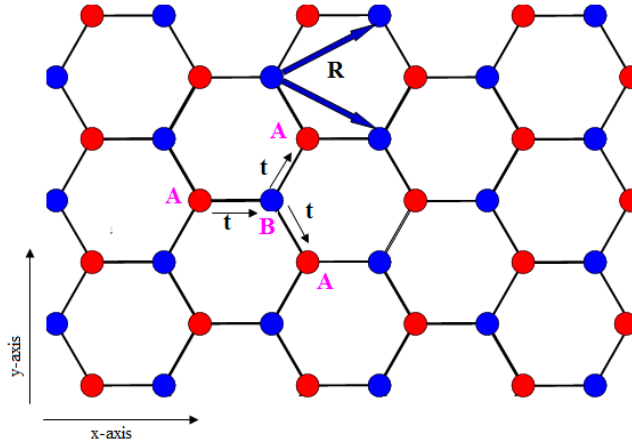


Figure 2.1: Honeycomb lattice with primitive vectors

and $R_{m,n} = m_1 a_1 + m_2 a_2$ is Bravais lattice vector where $(m_1, m_2) \in \mathbb{Z}$



There are three types of nearest neighbor bonds, namely [26],

1. Along the y axis with $\theta = \frac{\pi}{2}$
2. Along $\theta = \frac{\pi}{2} + \frac{2\pi}{3}$
3. Along $\theta = \frac{\pi}{2} + \frac{4\pi}{3}$

Then, total contribution to the Hamiltonian can be written as [26],

$$H = -t \sum a_{r_i}^\dagger b_{r_i+e_1} - t \sum a_{r_i}^\dagger b_{r_i+e_2} - t \sum a_{r_i}^\dagger b_{r_i+e_3} + h.c. \quad (2.2)$$

where,

$$\begin{aligned} \vec{e}_1 &= (0, a) \\ \vec{e}_2 &= \left(-\frac{\sqrt{3}}{2}a, -\frac{a}{2}\right) \\ \vec{e}_3 &= \left(\frac{\sqrt{3}}{2}a, -\frac{a}{2}\right) \end{aligned} \quad (2.3)$$

Now, we can perform Fourier transform by using following,

$$\begin{aligned} a_{r_i} &= \frac{1}{\sqrt{N}} \sum_k a_k e^{-i\vec{k}\cdot\vec{r}} \\ b_{r_i} &= \frac{1}{\sqrt{N}} \sum_k b_k e^{-i\vec{k}\cdot\vec{r}} \end{aligned} \quad (2.4)$$

Now, let us take,

$$\begin{aligned} -t \sum_i a_{r_i}^\dagger b_{r_i+\vec{e}_1} &= -\frac{t}{N} \sum_{i,k,k'} a_k^\dagger e^{i\vec{k}\cdot\vec{r}_i} b_{k'} e^{-i\vec{k}'\cdot(\vec{r}_i+\vec{e}_1)} \\ &= -t \sum_{k,k'} a_k^\dagger b_{k'} e^{-i\vec{k}'\cdot\vec{e}_1} \frac{1}{N} \sum_i e^{i\vec{k}-\vec{k}'\cdot\vec{r}_i} \\ &= -t \sum_{k,k'} a_k^\dagger b_{k'} e^{-i\vec{k}'\cdot\vec{e}_1} \delta_{k,k'} \\ &= -t \sum_k a_k^\dagger b_k e^{-i\vec{k}\cdot\vec{e}_1} \end{aligned} \quad (2.5)$$

Similarly,

$$\begin{aligned} -t \sum_i a_{r_i}^\dagger b_{r_i+\vec{e}_2} &= -t \sum_k a_k^\dagger b_k e^{-i\vec{k}\cdot\vec{e}_2} \\ -t \sum_i a_{r_i}^\dagger b_{r_i+\vec{e}_3} &= -t \sum_k a_k^\dagger b_k e^{-i\vec{k}\cdot\vec{e}_3} \end{aligned} \quad (2.6)$$

Now, taking Hermitian conjugate and insert in equation 2.3, we get,

$$\begin{aligned} H &= -t \sum_k a_k^\dagger b_k (e^{-i\vec{k}\cdot\vec{e}_1} + e^{-i\vec{k}\cdot\vec{e}_2} + e^{-i\vec{k}\cdot\vec{e}_3}) \\ &\quad -t \sum_k b_k^\dagger a_k (e^{i\vec{k}\cdot\vec{e}_1} + e^{i\vec{k}\cdot\vec{e}_2} + e^{i\vec{k}\cdot\vec{e}_3}) \end{aligned} \quad (2.7)$$



$$H = \sum_k \begin{bmatrix} a_k^\dagger & b_k^\dagger \end{bmatrix} \begin{bmatrix} 0 & -t(e^{-i\vec{k}\cdot\vec{e}_1} + e^{-i\vec{k}\cdot\vec{e}_2} + e^{-i\vec{k}\cdot\vec{e}_3}) \\ -t(e^{i\vec{k}\cdot\vec{e}_1} + e^{i\vec{k}\cdot\vec{e}_2} + e^{i\vec{k}\cdot\vec{e}_3}) & 0 \end{bmatrix} \begin{bmatrix} a_k \\ b_k \end{bmatrix}$$

(2.8)

Now using equation 2.3 and $\vec{k} = k_x\hat{i} + k_y\hat{j}$ we get,

$$\vec{k}\cdot\vec{e}_1 = k_y a$$

$$\vec{k}\cdot\vec{e}_2 = \frac{-\sqrt{3}}{2}k_x a - \frac{a}{2}k_y$$

$$\vec{k}\cdot\vec{e}_3 = \frac{\sqrt{3}}{2}k_x a - \frac{a}{2}k_y$$

Then, we get Hamiltonian matrix as,

$$H(k) = \begin{bmatrix} 0 & -t(e^{-ik_y a} + e^{i(\frac{\sqrt{3}}{2}k_x a + \frac{a}{2}k_y)} + e^{i(\frac{-\sqrt{3}}{2}k_x a + \frac{a}{2}k_y)}) \\ -t(e^{ik_y a} + e^{-i(\frac{\sqrt{3}}{2}k_x a + \frac{a}{2}k_y)} + e^{-i(\frac{-\sqrt{3}}{2}k_x a + \frac{a}{2}k_y)}) & 0 \end{bmatrix} \quad (2.9)$$

The eigenvalues of $H(k)$ gives the dispersion relation,

$$E(\vec{k})_{\pm} = \pm |t| \sqrt{3 + 2\cos(\sqrt{3}k_x a) + 4\cos(\frac{\sqrt{3}}{2}k_x a)\cos(\frac{3}{2}k_y a)} \quad (2.10)$$

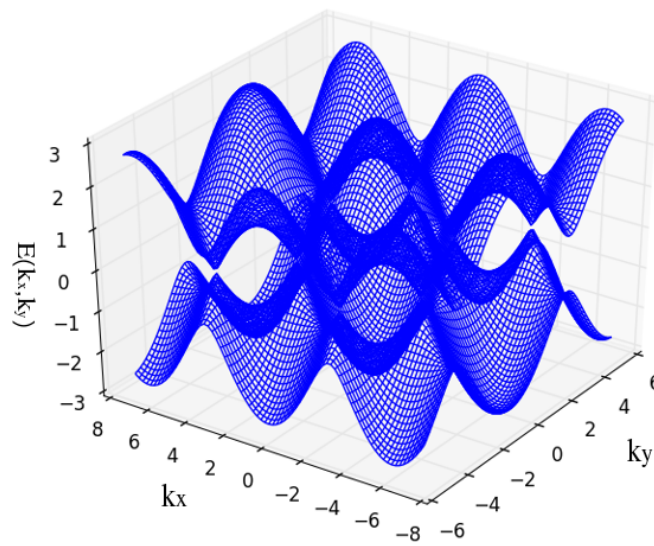


Figure 2.2: Energy-band diagram of honeycomb lattice.

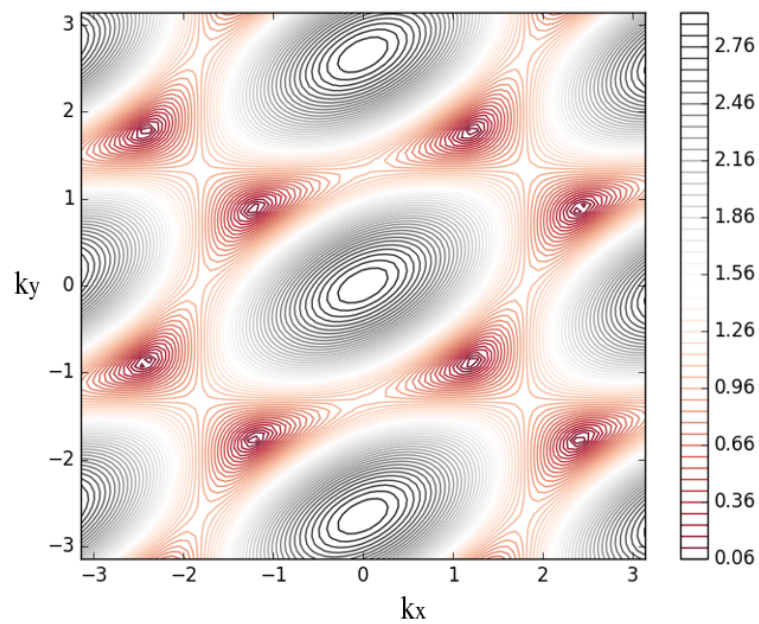


Figure 2.3: Contour plot of energy band for Honeycomb lattice

As we can see from the contour plot that, the energy dispersion is a periodic function of k -space i.e. hexagonal pattern repeats itself as shown in the figure. The first B.Z. is a hexagon.



2.2 Honeycomb lattice in a magnetic field

In the tight binding approximation, the hopping parameter are replaced by a Peierls substitution [2], [4],

$$t_{m,n} \rightarrow t_{m,n} e^{2i\pi\Phi_{m,n}} \quad (2.11)$$

where $\Phi_{m,n}$ is defined as line integral of the vector potential from site m to n ;

$$\Phi_{m,n} = -\frac{e}{\hbar} \oint_c \vec{A} \cdot d\vec{r} \quad (2.12)$$

So, with the magnetic flux through arbitrary area S in units of the magnetic quantum flux Φ_0 and A is vector potential. Here, vector potential A satisfy the condition that, integral $\oint_c \vec{A} \cdot d\vec{r}$ around the hexagonal unit cell equals the magnetic flux per unit cell, $\Phi_{m,n}$ [12].

For each lattice, we define the translational invariance along y direction with the x direction perpendicular. Here, we take particular choice of gauge where only one of the three $\Phi_{m,n}$ adjoining the nearest neighbour carbon pairs is set to be nonzero [15]. We define the magnetic unit cell as shown in figure below in such a way that, the area of magnetic unit cell becomes $q.S$, where q is the number of lattice site and S is the area of unit cell for a given value of $\Phi_{m,n} = \Phi = \frac{p}{q}$ [16]

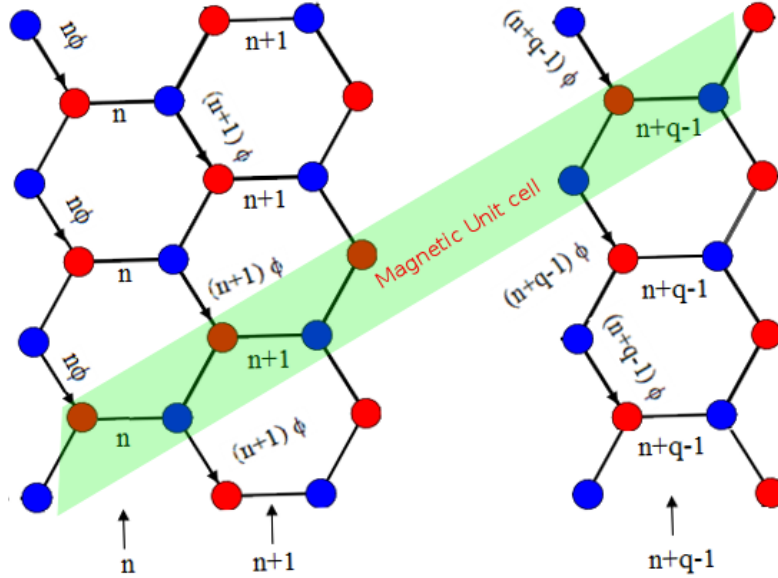


Figure 2.4: Magnetic unit cell in Honeycomb lattice

The diagram demonstrate the gauge used in the given lattice. The shaded part in the figure represent the magnetic unit cell. Different carbon sites with sublattice A and B within the same magnetic unit cell are denoted by the index ' n '. Here, one should note that two sublattice A and B connected horizontally have same index ' n '. The arrow shows the direction of non-zero phases



which are gained by Peierls substitution while all other phases are considered to be zero [16].

The tight binding Hamiltonian for graphene having 3 nearest neighbor in a constant magnetic field perpendicular to the plane is written as [15],

$$H = - \sum_{m,n} [e^{i\pi(\Phi)n} a^\dagger(m,n)b(m,n) + e^{-i\pi(\Phi)n} a^\dagger(m,n)b(m-1,n) + a^\dagger(m,n)b(m,n-1) + h.c.] \quad (2.13)$$

where, $a^\dagger(m,n)$ and $a(m,n)$ respectively creates and annihilates an electron at sites (m,n) on sublattice A . And similarly on sublattice B .

Now, to solve Schrodinger wave equation, a Fourier transformation for creation operator for the electrons in the system in the translational invariant direction is introduced as [14]

$$c_\alpha(m,n) = \frac{1}{\sqrt{N}} \sum_k e^{ikr_\alpha} d_k(m,n) \quad (2.14)$$

Then, by solving Schrodinger wave equation by defining a one particle state in terms of creation and annihilation operator, one can obtain the Harper's equation [16] as,

$$\begin{aligned} E\psi_{\alpha,n}^A &= \psi_{\alpha,n-1}^B + \psi_{\alpha,n}^B + e^{2\pi i n \Phi} \psi_{\alpha+1,n-1}^B \\ E\psi_{\alpha,n}^B &= \psi_{\alpha,n+1}^A + \psi_{\alpha,n}^A + e^{-2\pi i (n+1)\Phi} \psi_{\alpha-1,n+1}^A \end{aligned} \quad (2.15)$$

where, α denotes the position of a given magnetic unit cell along the y direction and the index ' n ' denotes position of each dimer within the magnetic unit cell.

These Harper's equations can be simplified by using the lattice translational symmetry along the y -direction. Here, α dependence can be removed by imposing Bloch's theorem,

$$\psi_{\alpha,n} = \psi_{n,\tilde{k}_y} e^{i\tilde{k}_y \alpha}$$

where, $\tilde{k}_y = k_y \sqrt{3}a$

Then, Harper equations are given as,

$$\begin{aligned} E\psi_{n,\tilde{k}_y}^A &= A_n(\tilde{k}_y)\psi_{n-1,\tilde{k}_y}^B + \psi_{n,\tilde{k}_y}^B \\ E\psi_{n,\tilde{k}_y}^B &= A_n^*(\tilde{k}_y)\psi_{n+1,\tilde{k}_y}^A + \psi_{n,\tilde{k}_y}^A \end{aligned} \quad (2.16)$$

where, $A_n(\tilde{k}_y) = 2e^{i(n\pi\Phi + \frac{\tilde{k}_y}{2})} \cos(n\pi\Phi + \frac{\tilde{k}_y}{2})$

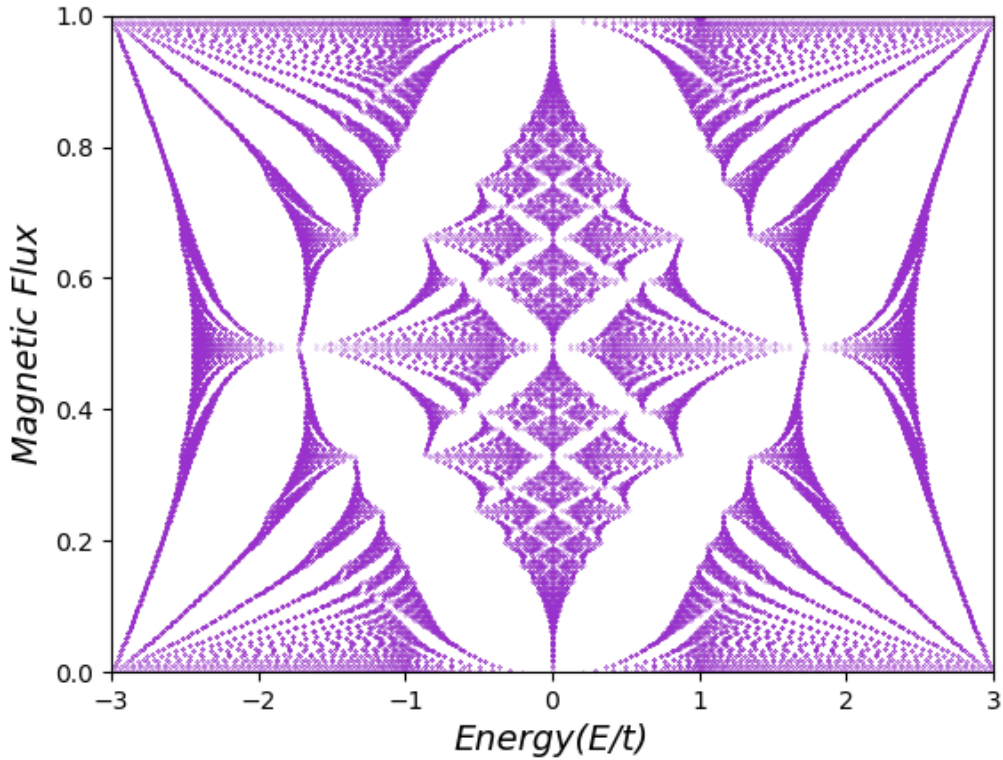


Figure 2.5: Hofstadter butterfly calculated for the Honeycomb lattice for $q=251$

This is the case where we have used hopping amplitude to be 1 and this hopping amplitude to all its neighbors are same. The magnetic flux is plotted vertically from 0 to 1, while energy is plotted horizontally from $-3t$ to $3t$.

The Hofstadter butterfly features an infinite number of gaps due to its fractal nature and closure of any one of these gaps creates a topologically different spectrum in principle [18].

2.4 Hofstadter butterfly in a tunable optical lattice

If we consider the case of tunable optical lattice, then we assume two hopping amplitude as shown in the figure,

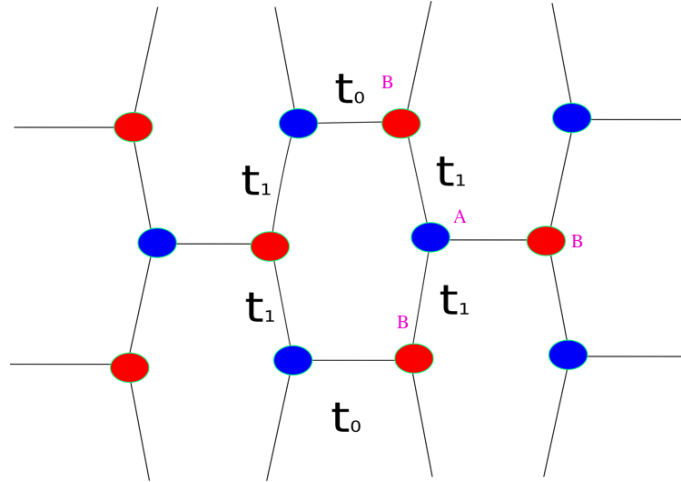


Figure 2.6: Tunable optical lattice

The tunneling amplitudes values t_0 and t_1 are taken to be $t_0 = 0.03488$ and $t_1 = 0.0843$ as discussed in reference [18]. Based on these parameter, we numerically solve the eigen value equation based on reference [18]. With the introduction of two hopping amplitudes , we get slightly different butterfly in comparison to the ideal honeycomb lattice.

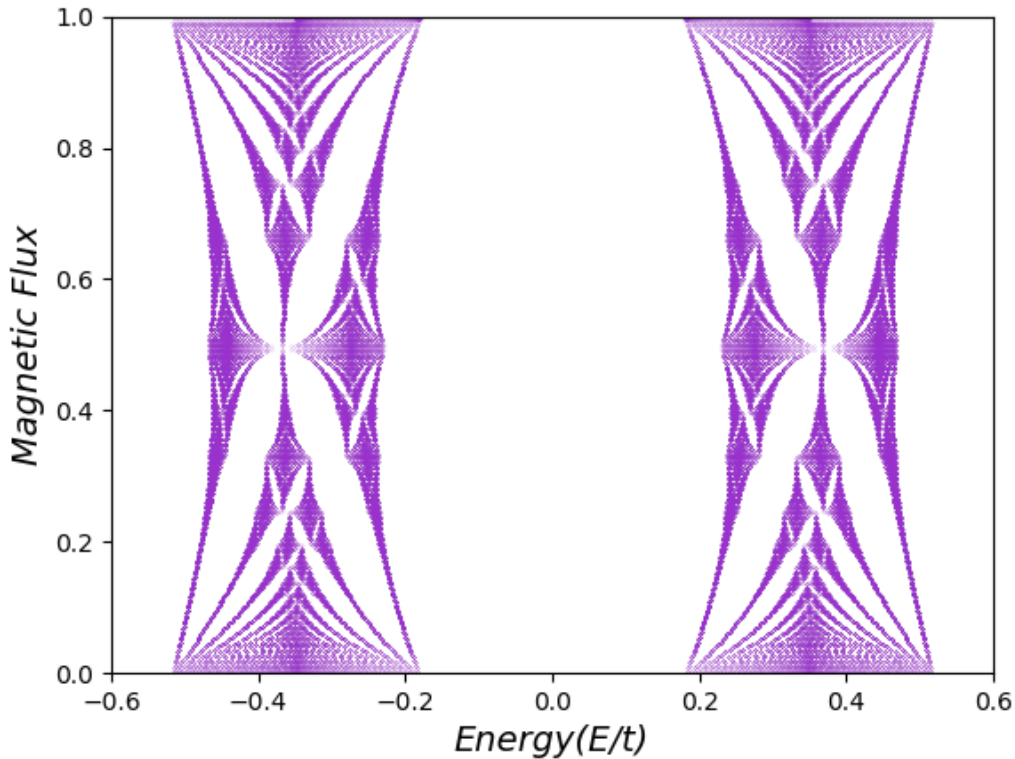


Figure 2.7: Hofstadter Butterfly in a Tunable lattice.

We can clearly see that, there exist a large gap around energy value $E = 0$ due to the difference in hopping amplitude. This energy spectrum is similar to two square lattice Hofstadter butterfly separated by a large gap. So, by adjusting the values of tunneling amplitude we can obtained the



energy spectrum for ideal honeycomb lattice. If we put the both the tunneling amplitude to be 1, and follow the procedure as describe in reference [18], then we obtained the same energy spectrum for honeycomb lattice that we discussed earlier.

Chapter 3

Berry Curvature, Berry Phase, Chern Number

3.1 Introduction

Next we are more interested in describing the topological behaviour of the lattices in the presence of magnetic field. Chern number is significant in describing such behaviour. In addition chern number is related with Berry curvature. In order to describe a Berry curvature let us consider the eigen function of the ν^{th} band as we discussed in Chapter 1,

$$u_\nu(k) = \begin{bmatrix} \psi_1^\nu(k) \\ \vdots \\ \psi_{q-1}^\nu(k) \end{bmatrix} \quad (3.1)$$

As we know vector potential is not a physical observable and its value depends on the choice of the gauge and the quantity with the physical meaning is the curl of it, which is the magnetic field [20]. We define a Berry curvature [19],

$$\Omega_\nu(k) = \nabla_k \times \langle u_\nu(k) | i \Delta_k | u_\nu(k) \rangle \quad (3.2)$$

Berry curvature is the curl of Berry connection and geometrical property of the band that only depends on its wave function and is a local gauge invariant [19].

We can also write as

$$\Omega_\nu(k) = \nabla_k \times A_\nu(k), \quad (3.3)$$

where, $A_\nu(k) = \langle u_\nu(k) | i \nabla_k | u_\nu(k) \rangle$, is Berry connection [20].

A physical interpretation of the Berry connection and curvature, is that they represent a magnetic vector potential and field in momentum space, as found by Berry [20], and discussed also by Price et al. [21]. By integrating the Berry connection around the closed path in B.Z. we obtained the phase called Berry phase [20].



$$\gamma_\nu = \oint_c \vec{A}_\nu(k) \cdot d\vec{k} \quad (3.4)$$

Here, one should note that Berry phase is gauge invariant [20].

Berry phase can be written as,

$$\gamma_\nu = \int_s \Omega_\nu(k) \cdot d\vec{S} \quad (3.5)$$

Where we have used stoke's theorem and S is the surface enclosed by contour c . We can interpret that Berry curvature plays the role of magnetic field in momentum space.

The integral of Berry curvature over Brillouin zone is an integer number and is called as chern number [22].

$$C_\nu = \frac{1}{2\pi} \int \Omega_\nu(k) \cdot \vec{e}_z dk_x dk_y \quad (3.6)$$

This has important consequence in the integer quantum Hall Effect.

3.2 Chern Number and Hall conductance

For all energy bands below the Fermi energy E_f are filled and Fermi energy lies within the gap, the Hall conductance is given as [8],

$$\sigma_{xy} = \frac{ie^2}{2\pi h} \sum_{E_{E_\nu} < E_f} \int \left(\left\langle \frac{\partial u_\nu(k)}{\partial k_x} \middle| \frac{\partial u_\nu(k)}{\partial k_y} \right\rangle - \left\langle \frac{\partial u_\nu(k)}{\partial k_y} \middle| \frac{\partial u_\nu(k)}{\partial k_x} \right\rangle \right) dk_x dk_y \quad (3.7)$$

where, $u_\nu(k)$ is eigenvector of $H(k)u_\nu(k) = E_\nu(k)u_\nu(k)$ of ν^{th} band E_ν and sum runs all over occupied bands below fermi energy and integral is taken over B.Z. The term in paranthesis represents Berry curvature of ν^{th} band [8].

Then Hall conductance in terms of chern number is given as,

$$\sigma_{xy} = \frac{e^2}{h} \sum_{E_{E_\nu} < E_f} C_\nu \quad (3.8)$$

One should note that, sum of the chern number of all bands must be zero because if all bands are occupied there are no conducting states available and Hall conductance is zero [19].

3.3 The Diophantine equation

Suppose three integers r, p and q where p and q are co-prime always satisfy the equation [32],

$$pt_r + qs_r = r \quad (3.9)$$



This is the diophantine equation where t_r and s_r are unknown. These values depend on r .

Note: Mathematically the equation has a solution for $t_r, s_r \in Z$ if and only if r is a multiple of greatest common divisor of p and q . 1 is the obvious greatest common divisor. This has a unique solution if,

$$\begin{aligned} 0 &\leq r \leq q \\ |t_r| &\leq \frac{q}{2} \end{aligned} \quad (3.10)$$

Dividing equation 3.9 by q , then we get,

$$\frac{r}{q} = \Phi_{AB} t_r + s_r \quad (3.11)$$

where, $\frac{r}{q} = n_e =$ density of states below r^{th} gap.

Another way to represent Hall conductance is [23],

$$\begin{aligned} \sigma_{xy} &= -e \frac{\partial n_e}{\partial \Phi} \\ &= -e \frac{\partial}{\partial \Phi} (\Phi_{AB} t_r + s_r) \\ &= -\frac{e^2}{h} t_r \end{aligned} \quad (3.12)$$

Where we have used, $\Phi_{AB} = \frac{\Phi}{\Phi_0}$ and $\Phi_0 = \frac{h}{e}$ So, Hall conductance is ,

$$\sigma_{xy} = -\frac{e^2}{h} t_r \quad (3.13)$$

where, $t_r \in Z$ is a solution of Diophantine equation. This expression is valid if we assume, density n_e is differentiable function of magnetic flux. Also, s_r and t_r are independent of magnetic field, which is true.

Chern number and Hall Conductance in Hofstadter butterfly

Comparing equations for Hall conductance 3.8 and 3.13 which is obtained from diophantine equation, we get,

$$t_r = -\sum_{\nu=1}^r C_\nu \quad (3.14)$$

This equation means that, in Harper-Hofstadter model, to each q band we can associate a topological invariant number, C_ν such that equation 3.14 is solution of Diophantine equation.

With this relation Hofstadter butterfly gets its colour according to the quantized values of the Hall conductance, t_r . Using such a simple argument we can calculate the Hall conductance and the Chern number of all the Harper-Hofstadter bands. The same results can be also obtained



numerically [8], following the method proposed by Fukui [24]. This method relies on the calculation of the Berry curvature from the eigenvectors of equation 3.1.

Now, let us consider the case where $\Phi = \frac{1}{3}$. For this value, clearly we have $p = 1$ and $q = 3$. As we discussed earlier, for the unique solution of diophantine equation, it should satisfied the relation, $0 \leq r \leq q$ and $|t_r| \leq \frac{q}{2} \leq 3$ and $|t_r| \leq \frac{3}{2}$. With this conditon we must have, $r \leq 3$. So, $-\frac{3}{2}t_r \leq \frac{3}{2}$, and since, $t_r \in \mathbb{Z}$ we get, $t_r = 0, \pm 1$.

If $r=1$, using diophantine equation 3.9, we get $t_r = 1$ and $s_r = 0$. Since, $t_r = -\sum_{\nu=1}^r C_\nu$, this implies, $C_1 = 1$.

For $r=2$, $t_r = -1$ and $s_r = 1$ and $C_1 + C_2 = 1$

For $r=3$, $t_r = 0$ and $s_r = 1$ and $C_1 + C_2 + C_3 = 0$

Then, we have, $C_1 = 1, C_2 = 2, C_3 = -1$. Now, by calculating the chern number we can calculate the Hall conductance by using the equation 3.13 .

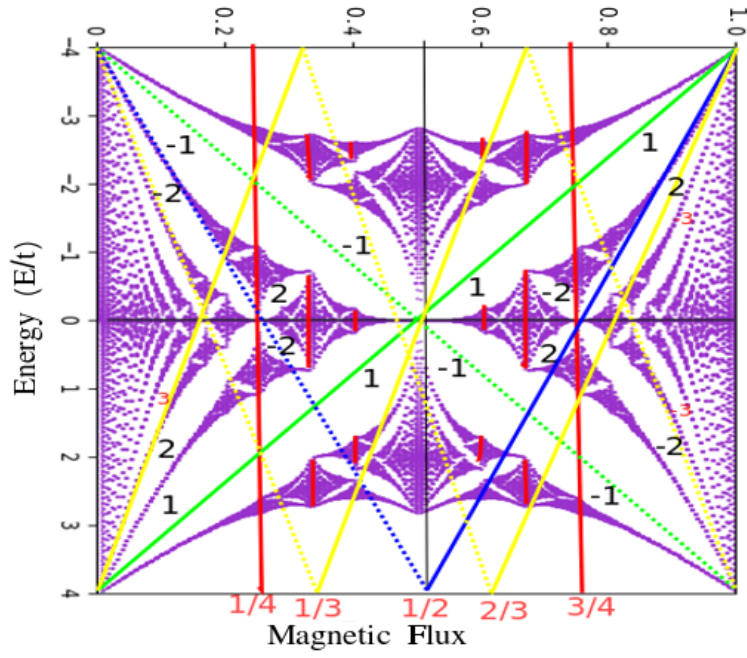


Figure 3.1: Chern number representation in square Hofstadter butterfly at different values of Φ . The x -axis represents magnetic flux and y -axis represents Energy.

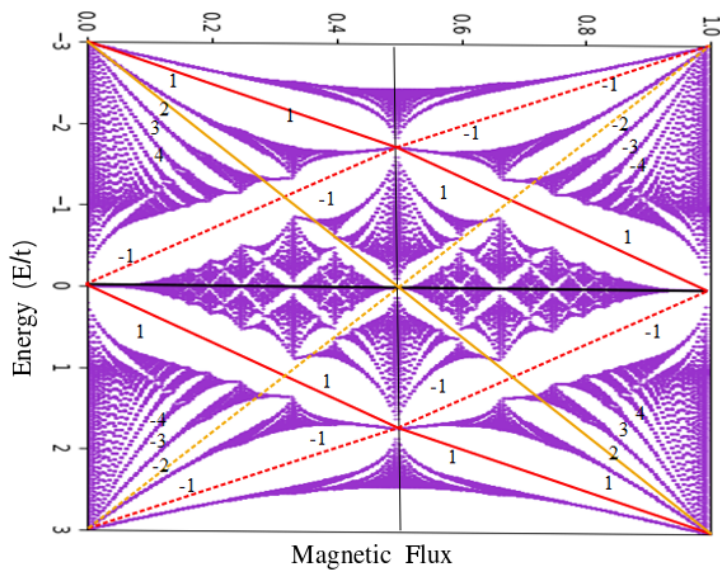


Figure 3.2: Chern Number representation in honeycomb Hofstadter butterfly at different values of Φ . The y -axis represents magnetic flux and x -axis represents Energy.

Chapter 4

Future Work

In the presence of magnetic field, electrons change its path and move in curve direction and gets accumulated at a certain place. Meanwhile, there exist holes in opposite direction and create a voltage. This is Hall effect [25]. In general, hall conductance is proportional to magnetic field [27] but at low temperature it is not the case [28].

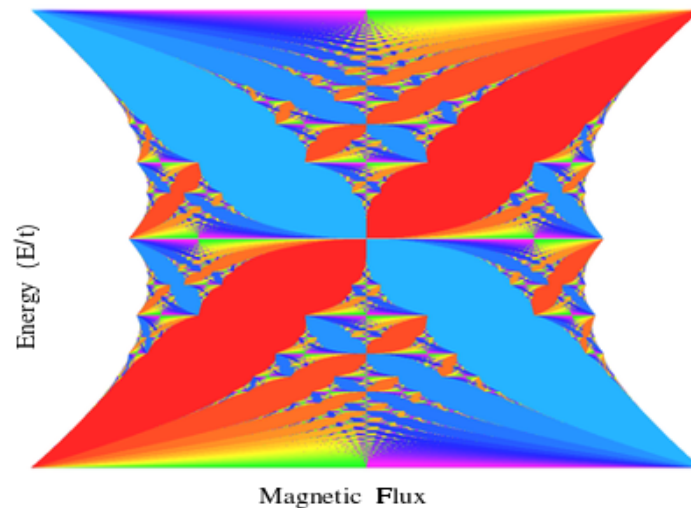


Figure 4.1: The colored butterfly, [29], shows energy gaps colored according to the quantized values of the Hall conductance. Warm colors indicate positive chern numbers, and cool colors negative. The x -axis represents magnetic flux and y -axis represents Energy.

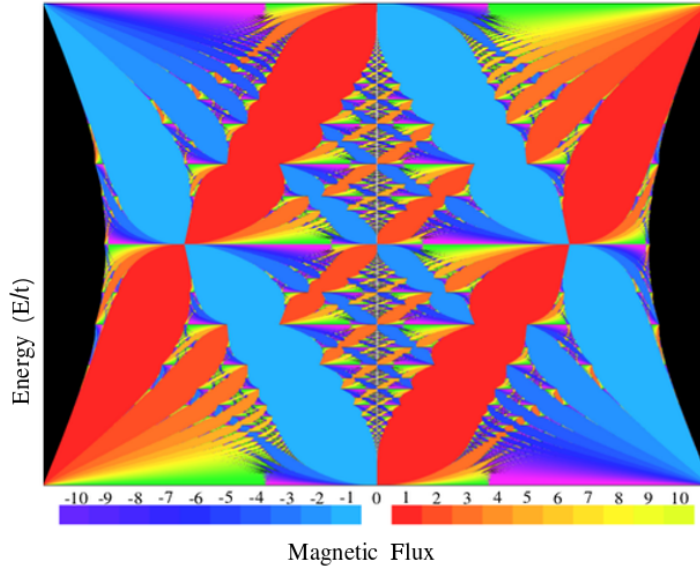


Figure 4.2: The colored butterfly, [30], shows energy gaps colored according to the quantized values of the Hall conductance. Warm colors indicate positive Chern numbers, and cool colors indicate negative. The x -axis represents magnetic flux and y -axis represents Energy.

The existence of Landau levels leads to a quantized Hall conductance and is known as the quantum Hall effect, discovered by K.V.Klitzing, G.Dorda, and M.Pepper in 1980 [27]. At low temperature, the variation of conductance with the magnetic field is not linear rather there are lots of plateaus appear [28]. At these plateaus, conductance is quantized to integer values and these plateaus are known as Integer Quantum Hall effect [15].

Each color corresponds to a value of conductance (integer number of conductance quanta) that remains constant in the same energy gap. The Hall conductance in the presence of a magnetic field is quantized as a function of the number of Landau levels. As we discussed earlier, each gap in butterfly has unique chern number and that chern number corresponds to Hall conductance. Due to gauge invariance, conductance is quantized as integer multiples of e^2/h and only changes when the Fermi level shifts from one gap to another [31]. In the case of the butterfly, landau levels are split in sub-levels in the presence of magnetic field. This section describes the behavior of the conductance in the subbands [32].

So far, for the study of Hall conductance, we reviewed some of the important papers that has been published, and give general idea about the conductance. In future, we can use this thesis as a reference to calculate colored Hofstadter Butterfly numerically and go in depths for the detailed explanation of Integer Quantum Hall Effect in case of square and honeycomb lattice. It would be interesting to extend this approach in the case of next nearest neighbour consideration and see the effect on Integer Quantum Hall Effect.

Summary

The main aim of this thesis is to discuss how two dimensional lattices behaves in magnetic field. We have provided the theoretical framework and some of the numerical calculations in order to demonstrate the effect on square lattice and honeycomb lattice. In order to describe the sysetm we have used tight binding model. While considering the effect of magnetic field we make use of Peierls substitution. The generating vector potential is chosen similar to the usual Landau gauge such that phase can be altered along x and y direction. The idea of magnetic translation operators has been used in order to make possible to diagonalize the Hamiltonian in the presence of homogeneous magnetic field. With inclusion of homogeneous magnetic field, we have used the concept of magnetic unit cell which preserve the transaltion invariance which was broken in regular unit cell. The choice of magnetic unit cell is independent. It can be used along x -direction or y -direction.

At first, eigen values are calculated mathematically in the absence of magnetic field for both of the square and honeycomb lattices. Later, in the presence of magnetic field, eigen values are calculated numerically. By plotting the eigen values against rational magnetic flux, it results beautiful but complicated energy spectrum diagram which is known as Hofstadter Butterfly. We can relate the structure of butterfly with the help of chern number. When value of magnetic flux is rational $\Phi = \frac{p}{q}$, then the energy band generally known as Landau level, splits into q bands having $q-1$ band gap.

Each gap in between the energy level can be explained by topological invariant number known as chern number with the help of Berry connection and Diophantine equation. Each gap has its own chern number and remains same throughout that gap. In going from one band to other band gap, i.e. by crossing the landau level, chern number will be different. With Diophantine equation, we can know that chern number is related with Hall conductance. So, if we are able to calculate chern number then we will be able to calculate the Hall conductance also.

Calculation of chern number numerically and hence calculating the Integer Quantum Hall coductance can be done as a future work. From here we can extend our work to go in details about Integer quantum Hall effect. So far, we did calculation by cosidering nearest neighbour approach. It would be interesting to see how Hofstadter butterfly behaves if we consider next neighbour approach and equally at the same time the variation in Integer Quantum Hall Effect.

Bibliography

- [1] Monika Aidelsburger, Artificial gauge fields with ultracold atoms in optical lattices, Springer(2016)
- [2] R. E. Peierls, Z. Phys.80,763(1933)2-4
- [3] Aharonov–Bohm effect *Retrived from* : https://en.wikipedia.org/wiki/Aharonov-Bohm_effect
- [4] D. R. Hofstadter, Energy levels and wave functions of Bloch electrons in rational and irrational magnetic fields, Phys.Rev.B 14,2239(1976)1-3
- [5] M. Y. Azbel, Energy spectrum of a conduction electron in a magnetic field. JETP 19(1964)
- [6] P. G. Harper, Single band motion of conduction electrons in a uniform magnetic field. Proc. Phys.Soc., A 68:874,(1955)5,8
- [7] F. Yilmaz, F. Nur Unal and M. O. Oktel, Evolution of the Hofstadter butterfly in a tunable optical lattice, *Department of Physics, Bilkent University, Turkey*,(2015)1-9
- [8] G. Salerno, *PhD thesis: Artificial Gauge Fields in Photonics and Mechanical Systems*(2016)1-15
- [9] E. Brown, Bloch electrons in a uniform magnetic field, Phys.Rev133(1964)1038-1044
- [10] J. L. Verbena, Density of states in the tight binding, *Master Thesis: Density of states in the tight binding model, Universidad Autonoma de Zacatecas*,(2007)6
- [11] P. R. Wallace, The band theory of graphite. Phys. Rev. 71(1947)622–634
- [12] R. P. Feynman, Lectures on Physics Vol.III(Addison-Wesley, New York(1965)).
- [13] F. Yilmaz, Evolution of the Hofstadter butterfly in a tunable optical lattice *Master thesis, Graduate school of engineering and science of bilkent university, Turkey*(2015)1-22
- [14] M. Sullivan, Tight-binding model for graphene, Phys 40182, The University of Manchester(2017)16
- [15] Castronetro
- [16] J. W. Rhim and K. Park, Self-similar occurrence of massless Dirac particles in graphene under a magnetic field, Phys.Rev.B 86, 235411(2012)



- [17] R. Rammal, Landau level spectrum of bloch electrons in a honeycomb lattice, *J. Phys. France*,46,(1985)45-54
- [18] F. Yilmaz, F. N. Unal and M.O. Oktel, Evolution of the Hofstadter butterfly in a tunable optical lattice,*Department of Physics, Bilkent University, Turkey*,(2015)1-6
- [19] D. Xiao, M. C. Chang, and Q. Niu. Berry phase effects on electronic properties. *Rev. Mod. Phys.*, 82:1959,(2010)11,13
- [20] M. V. Berry, Quantal phase factors accompanying adiabatic changes. *Proc. R. Soc. A*, 392:45,(1984)11
- [21] H. M. Price, T. Ozawa, and I. Carusotto, Quantum mechanics with a momentum-space artificial magnetic field. *Phys. Rev. Lett.*, 113:190403,(2014)11
- [22] Y. Aharonov and D. Bohm, Significance of electromagnetic potentials in the quantum theory. *Phys. Rev.*, 115:485,(1959)7
- [23] P. Strěda, Quantised Hall effect in a two-dimensional periodic potential, *J. Phys. C: Solid State Phys.*, 15:L1299,(1982)13
- [24] T. Fukui, Y. Hatsugai, and H. Suzuki, Chern numbers in discretized Brillouin zone: efficient method of computing (spin) Hall conductances. *J. Phys. Soc. Jpn.*, 74:1674,(2005)15
- [25] Topological insulators PartI, Lecture note *Retrived from <http://www-personal.umich.edu/~sunkai/teaching/Fall2013/chapter1.pdf>*
- [26] Topological Tight Binding models, Lecture note *Retrived from <http://www-personal.umich.edu/~sunkai/teaching/Fall2013/chapter6.pdf>*
- [27] K. V. Klitzing et al., New Method for high-accuracy determination of the fine-structure constant based on quantized Hall resistance, *Phys. Rev. Lett.* 45(1980).
- [28] N. Goldman, Characterizing the Hofstadter butterfly's outline with Chern numbers, *J. Phys. B: At. Mol. Opt. Phys.* 42(2009)
- [29] J. E. Avron. Multiscale Methods in Quantum Mechanics. Chapter 2: Colored Hofstadter butterflies, *Birkhäuser Boston*,(2003)14
- [30] A. Agazzi, J.-P. Eckmann and G.M. Graf, The Colored Hofstadter Butterfly for the Honeycomb Lattice, *Journal of Statistical Physics*,(2014)
- [31] R. B. Laughlin, Quantized Hall conductivity in two dimensions, *Phys. Rev. B* 23, 5632 (1981)
- [32] N. M. OREAU, Development of a tight-binding model to study Hofstadter's butterfly in graphene on h-BN exhibiting a moiré pattern. *Master Thesis : École polytechnique de Louvain (EPL)*,(2016)23